NORSAR

ROYAL NORWEGIAN COUNCIL FOR SCIENTIFIC AND INDUSTRIAL RESEARCH

NORSAR Scientific Report No. 2-86/87

SEMIANNUAL TECHNICAL SUMMARY

1 October 1986 - 31 March 1987

L.B. Loughran (ed.)

Kjeller, May 1987

VII.4 Multiple scattering by topographic relief

Wavenumber analysis of NORESS array data has revealed sometimes significant frequency dependent effects. Motivated by these phenomena we have developed a method to account for multiple scattering due to topography of internal boundaries or of the free surface. The method was originally developed for the in comparison simple problem of electromagnetic scattering by a perfectly conducting rough surface, and it is based on the so-called extinction theorem (e.g., Brown, 1985). The result is an approximation since it is given by a perturbation series whose terms are obtained recursively, but the method can be applied to any surface topography, the only restriction being implied by the condition of convergence of the series solution. The Born approximation is simply the first term of the series; it is thus straightforward to make a comparison with previous single scattering results. Here we present results of a comparative study of a rough solid-liquid boundary where explicit single scattering results are available (Doornbos, 1978). Topographic effects of the free surface and of solid-solid interfaces will be considered in later contributions.

The solid-liquid interface forms a relatively complicated problem due to the modified boundary conditions. Let the deviation of the interface from a plane be given by $z = f(x,y)$, hence the reference plane is taken to be the $z = 0$ plane in a cartesian coordinate system. The simplest form of interfacial displacement-traction vector needed to determine the scattered field is

$$\underline{d} = (u_x{}^+,\ u_y{}^+,\ \underline{\nu}^T\underline{u},\ \underline{\nu}^T\underline{\underline{\tau}}\,\underline{\nu}\ /\|\underline{\nu}\|^2)^T \qquad (1)$$

Here the solid is taken above the interface, i.e., u_x^+ and u_y^+ are the horizontal displacement components in the solid. The vector $\underline{\nu}$ is normal to the interface:

$$(\nu_x, \nu_y, \nu_z) = (-\frac{\partial f}{\partial x}, -\frac{\partial f}{\partial y}, 1)$$

hence $\underline{\nu}^T \underline{\underline{\tau}} \underline{\nu}$ is the normal traction, and $\underline{\nu}^T \underline{u}$ is a constant times the normal displacement component. The solution for $\underline{d}$ can be obtained recursively in wavenumber space. Let $\underline{\tilde{D}}(k_x,k_y)$ be the Fourier transform of $\underline{d}(x,y)$, and let

$$\underline{\tilde{D}}(k_x,k_y) = \sum_{n=0}^{\infty} \underline{\tilde{D}}^{(n)}(k_x,k_y) \tag{2}$$

then $\underline{\tilde{D}}^{(n)}$ is determined from $\underline{\tilde{D}}^{(n-m)}$, $m = 1,\ldots,n$. The details of this solution for an incident plane wave are given elsewhere (manuscript in preparation). The scattering coefficients $\underline{B}^{(n)}$ are similarly determined from $\underline{\tilde{D}}^{(n-m)}$, $m = 0,1,\ldots,n$, and the total scattered field is

$$\underline{B}(k_x,k_y) = \sum_{n=0}^{\infty} \underline{B}^{(n)}(k_x,k_y) \tag{3}$$

The components of $\underline{B}^{(0)}$ are just the plane wave reflection and transmission coefficients for a plane interface, $\underline{B}^{(0)}$ is the Born approximation representing single scattering, and $\underline{B}^{(n)}$, $n \geqslant 2$, include multiple scattering. From the components of $\underline{B}$ we can a.o. calculate the energy flux for any wave type j. Per unit of solid angle:

$$E_j(\theta,\phi) \sim \left(\frac{\omega^2}{v_j^2} - k_x^2 - k_y^2 \right)^{\frac{1}{2}} |B_j(k_x,k_y)|^2 \qquad (4)$$

where

$$(k_x,k_y) = \frac{\omega}{v_j} (\sin\theta \cos\phi, \sin\theta \sin \phi)$$

and v_j is the wave velocity.

The following examples are for a velocity-density structure:

$\rho^+ = 5.56$ g/cm^3, $\rho^- = 9.93$ g/cm^3, $\alpha^+ = 13.64$ km/s, $\alpha^- = 8.08$ km/s,
$\beta^+ = 7.2$ km/s, $\beta^- = 0$,

a space-stationary roughness function $f(x,y)$ characterized by a Gaussian autocorrelation:

$$r(x,y) = h^2 \exp\left(- \frac{x^2+y^2}{\sigma^2} \right)$$

and a lateral scale length $\sigma = 20$ km for 1 Hz waves: $\omega = 2\pi$ c/s. Fig. VII.4.1 illustrates the complete series solution for incident and scattered wave directions which are typically observed, and for different topographic height h. In the same figure we show the phase of the scattered wave due to a single bump with the same autocorrelation as the space-stationary roughness function. The first order phase solution is significantly biased. The bias turns out to be significant for topographic height above a few hundred meters. On the other hand, the first order approximation predicts the scattered energy remarkably well even for rather high topography (h = 3 km). Two other intuitively obvious features are: (1) The low order solutions are relatively stable for wave types and in wave directions where scattering is relatively strong, and (2) the higher order terms serve to enhance energy relatively far from the specular direction and to reduce energy near the specular direction. This is consistent with the fact that multiple scattering tends to widen the wavenumber spectrum of the scattered field. The difference between the first and higher order solutions becomes particularly pronounced in directions where the scattered field is relatively small, for example, near a zero of the reflection coefficient. Fig. VII.4.2 illustrates this phenomenon in the slowness range above 3 s/deg.

D.J. Doornbos

REFERENCES

Brown, G.S. (1985): A comparison of approximate theories for scattering from rough surfaces. Wave Motion, 8, 155-205.

Doornbos, D.J. (1978): On seismic wave scattering by a rough core-mantle boundary. Geophys. J.R. astr. Soc., 53, 643-662.

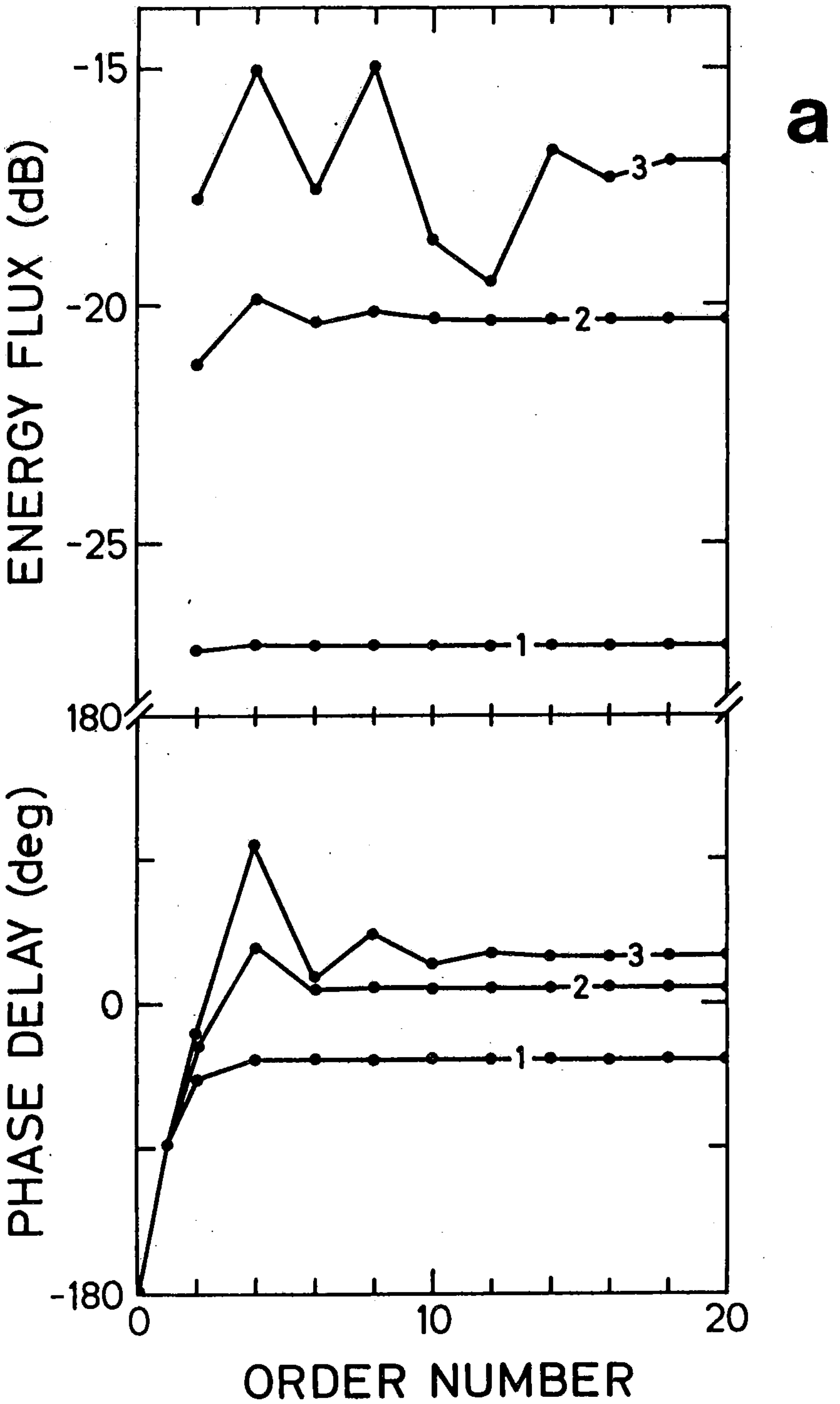

Fig. VII.4.1 (a) Energy flux and phase delay of scattered wave at 1 Hz, for subsequent orders of the series solution. Solid-liquid interface with velocity-density structure given in the text. The boundary roughness parameters are σ = 20 km and h = 1 km (1), 2 km (2), 3 km (3). Scattered P in the liquid from incident P in the liquid. The incident and scattered ray parameters are both 2.43 s/deg. The vertical planes through the incident and scattered rays differ by 44 degrees.

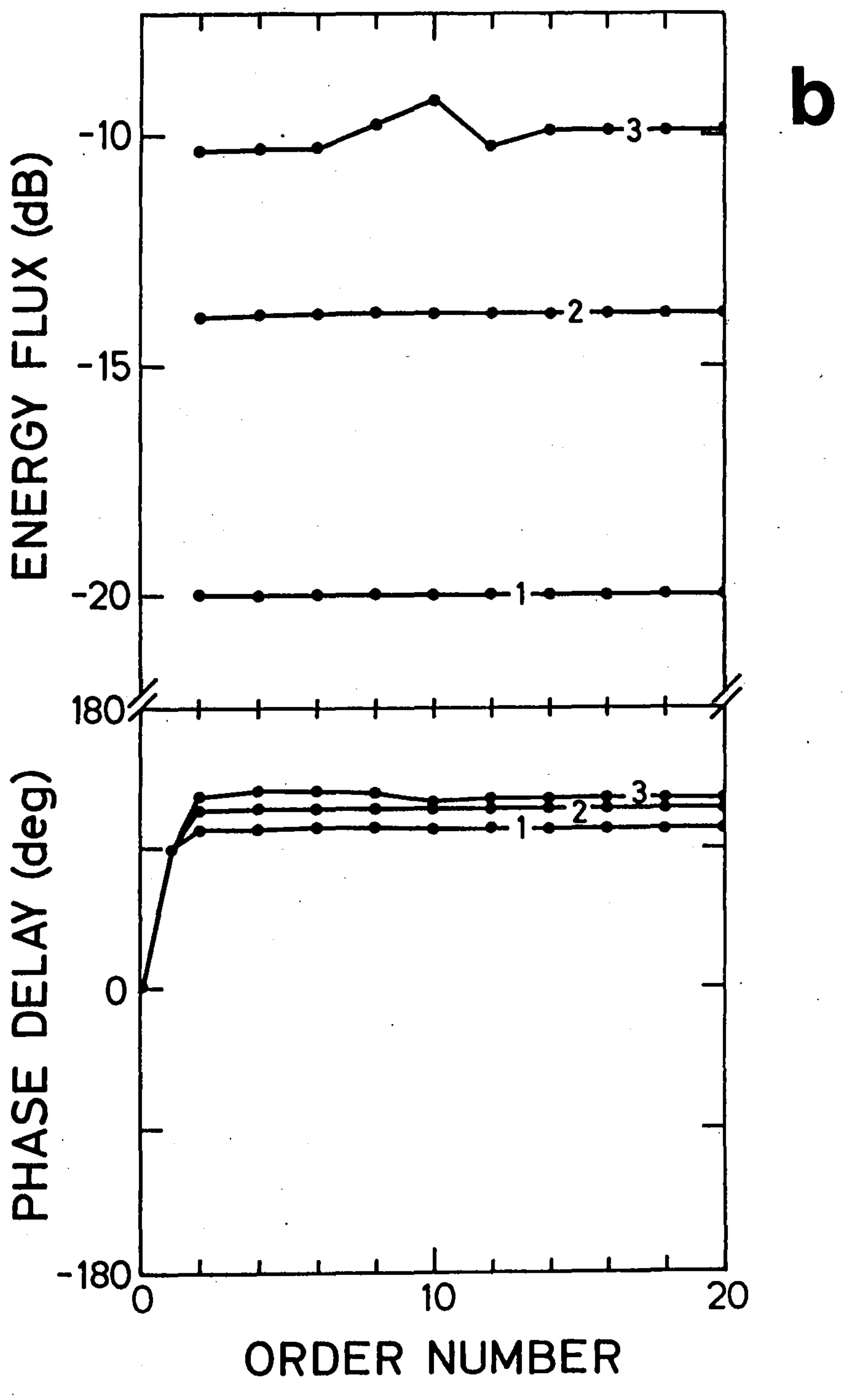

Fig. VII.4.1 (b) Scattered P in the solid from incident P in the liquid. Other details as in Fig. VII.4.1a.

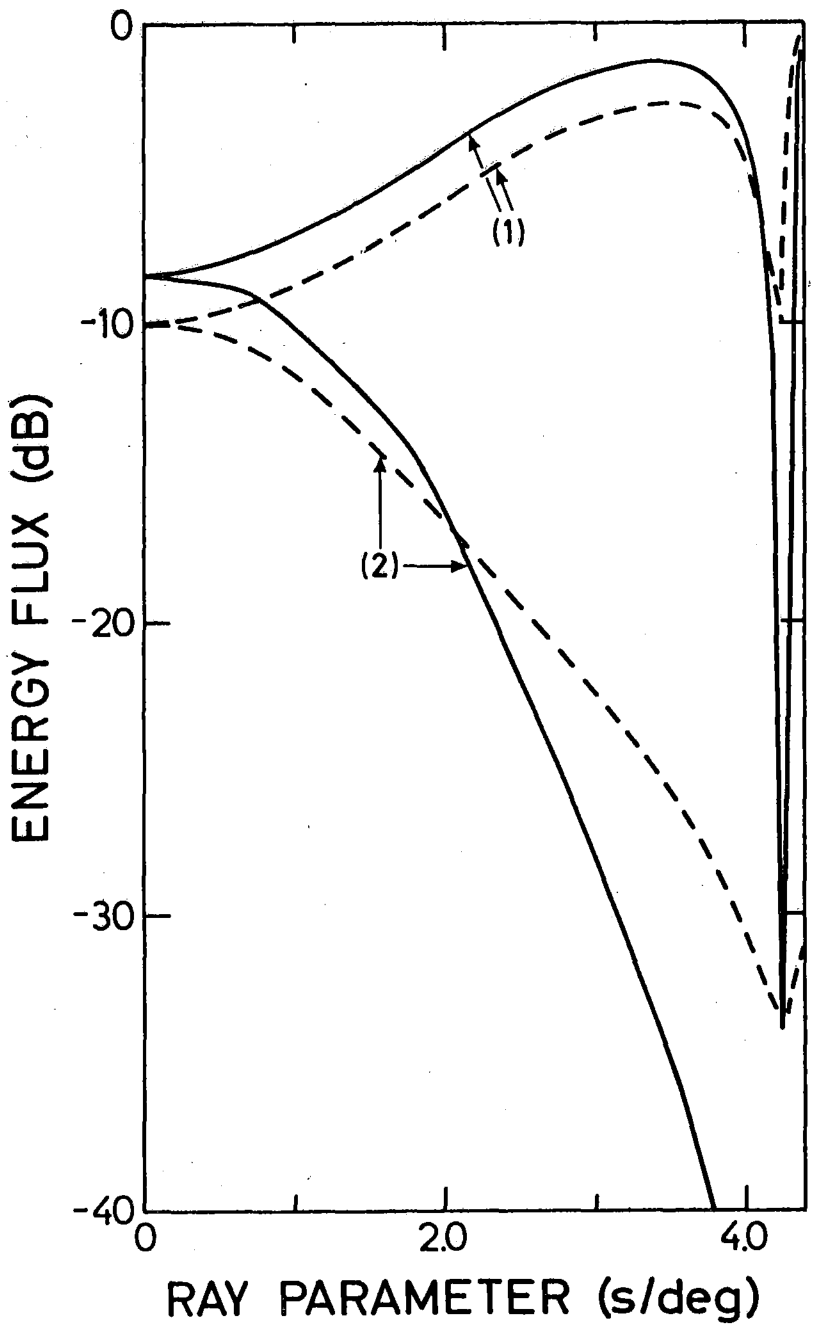

Fig. VII.4.2 Energy flux at 1 Hz through solid-liquid interface with the same specifications as in Fig. VII.x.1, and h = 2 km. Scattered P in the liquid from incident P in the liquid. The incident and scattered ray parameters are equal. (1): Specular direction. (2): The vertical planes through the incident and scattered rays differ by 44 degrees. Solid lines: first order approximation. Dashed lines: complete solution.